

## NOVEL METHODS FOR AXIAL FAN IMPELLER GEOMETRY ANALYSIS AND EXPERIMENTAL INVESTIGATIONS OF THE GENERATED SWIRL TURBULENT FLOW

by

**Zoran D. PROTIĆ<sup>†</sup>, Miloš S. NEDELJKOVIĆ<sup>a</sup>, Djorđe S. ČANTRAK<sup>a\*</sup>,  
and Novica Z. JANKOVIĆ<sup>b</sup>**

<sup>a</sup> Faculty of Mechanical Engineering, University of Belgrade, Belgrade, Serbia

<sup>b</sup> Innovation Center, Faculty of Mechanical Engineering, University of Belgrade, Belgrade, Serbia

Original scientific paper  
UDC: 621.634.001/.004  
DOI: 10.2298/TSCI100617025P

*Geometry analysis of the axial fan impeller, experimentally obtained operating characteristics and experimental investigations of the turbulent swirl flow generated behind the impeller are presented in this paper. Formerly designed and manufactured, axial fan impeller blade geometry (originally designed by Prof. Dr-Ing. Z. Protić<sup>†</sup>) has been digitized using a three-dimensional scanner. In parallel, the same impeller has been modeled by beta version software for modeling axial turbomachines, based on modified classical calculation. These results were compared. Afterwards, the axial fan operating characteristics were measured on the standardized test rig in the Laboratory for Hydraulic Machinery and Energy Systems, Faculty of Mechanical Engineering, University of Belgrade. Optimum blade impeller position was determined on the basis of these results. Afterwards, impeller with angle 22°, without outlet vanes, was positioned in a circular pipe. Rotational speed has been varied in the range from 500 till 2500 rpm. Reynolds numbers generated in this way, calculated for axial velocity component, was in the range from  $0.68 \cdot 10^5$  till  $2.5 \cdot 10^5$ . Laser Doppler anemometry measurements and stereo particle image velocimetry measurements of the three-dimensional velocity field in the swirl turbulent fluid flow behind the axial fan have been performed for each regime. Obtained results point out extraordinary complexity of the structure of generated three-dimensional turbulent velocity fields.*

Key words: axial fan, turbulence, swirl flow, PIV, LDA, 3-D scanning, modeling

### Introduction

Investigation of the axial fan geometries, their in built and operating characteristics, and turbulent swirl flow generated following the axial fan impeller have been occupying researchers attention for years. Though most of the operating characteristics have been cleared

---

\* Corresponding author; e-mail: [djcantrak@mas.bg.ac.rs](mailto:djcantrak@mas.bg.ac.rs)

out, still fundamentals of the generated swirl fluid phenomena stay undiscovered. Focus of this paper is on this very complex physical phenomenon and recent techniques in modeling modern blade geometries and revealing existing ones.

Originally designed and manufactured axial fan, by Protić<sup>†</sup> (figure 1), draw attention as it has good operating characteristics, interesting complex geometry and it was designed following the law  $rW = const$ . This geometry was a test example for beta version software for modeling axial turbomachines, based on modified classical calculation.

Revealing of this geometry was done in few steps. First step was laser 3-D scanning with ZScanner 700, followed by modeling in software CATIA. In the next step scanned and refined geometry was compared to the axial fan generated in new software.

Here are also presented results of testing the defined axial fan. Operating characteristics were obtained on the standardized test rig in the Laboratory for Hydraulic Machinery and Energy Systems, Faculty of Mechanical Engineering, University of Belgrade.

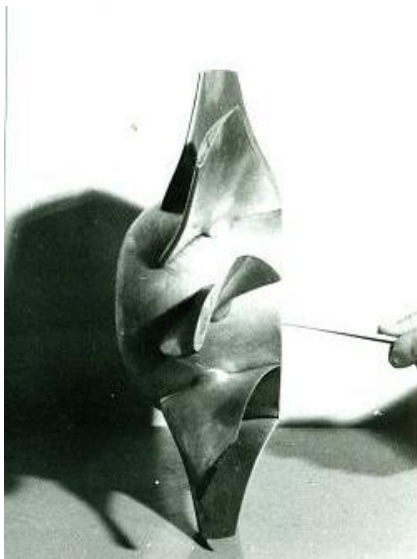


**Figure 1. Originally designed axial fan, by Protić<sup>†</sup>**

Fan was designed to work with outlet vanes (downstream guide wheel) and it was tested with them. Three types of outlet vanes were tested in combination with three impeller blade angles ( $\beta_R$ )  $22^\circ$ ,  $26^\circ$  and  $30^\circ$ , providing nine different combinations. Optimum fan blade position and stay vane type was determined on the basis of these results.

The third part of this work was investigation of the turbulent swirl flow phenomena behind the axial fan. It was done without outlet vanes, but with the impeller blade position  $\beta_R=22^\circ$ . Turbulent swirl flow fields were generated for various rotational speeds varied in the range from 500 till 2500rpm. Reynolds numbers, generated in this way, calculated for the axial velocity component, were in the range from  $0.68 \cdot 10^5$  till  $2.5 \cdot 10^5$ . LDA (laser Doppler anemometry) measurements and stereo PIV (Particle Image Velocimetry) measurements of 3-D velocity field in the swirl turbulent fluid flow behind the axial fan have been performed for each regime.

Various authors studied problem of swirl turbulent flows and formed, unofficially called, Belgrade school of turbulent swirl flows. Problem of defining dead water radius in swirl turbulent flow in straight circular pipes was studied by Protić [1]. Pressure and velocity fields, in order to study the turbulent swirl flow field, have been obtained with classical probes in various measuring sections along the test rig [2, 3]. Turbulent swirl flow field was also investigated, by use of hot-wire anemometry [4,5]. Many other authors with their significant papers left trace in this investigation [6, 7].

All these results point out extraordinary complexity of the structure of generated three dimensional turbulent velocity fields.

### 3-D scanning and modeling

#### *3-D scanning and reverse engineering*

Axial fan real geometry was captured by use of mobile scanner type ZScanner 700, manufacturer Z Corporation. It has XY accuracy of up to 50 microns, resolution 0.1 mm in Z direction, sampling speed is 18000 measurements/second, exported file formats are *.stl*, *.txt* and others. These exported file formats are very suitable for importing into CATIA software.

Randomly placed reflective registration targets, at maximum distance of 2cm, are distributed all over the scanned blade. Scanner is calibrated on defined target previous to measurements. Afterwards, software recognizes surface on the basis of three scanned markers. By moving scanner over the surface other surfaces have been recognized. Polygon mesh of the scanned object is formed in the real time (figure 2a). Scanner resolution is adjustable during operation. Each of them has a unique position, *i. e.* x-, y-, and z-coordinate, what lets the scanner recognize where it is relative to other dots. For detailed analysis of scanned data Geomagic Software was used. It generates file formats *.stl*, *.txt*, and other.

Hub geometry was scanned by use of specially designed mechanical device. Afterwards scanned impeller blade and hub were assembled in CATIA software (figure 2b). External diameter of an axial rotor is 0.398m, while dimensionless ratio of hub and external diameter is 0.5. Impeller has nine blades. It is a variable pitch fan.

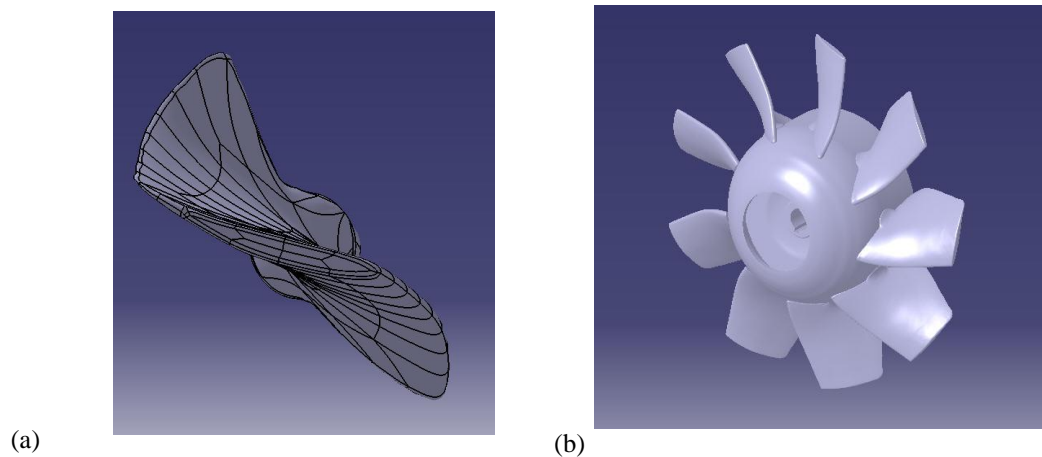


**Figure 2. a) Scanned impeller blade. Imported to the software CATIA; b) Modeled axial fan impeller geometry**

It is possible now to verify the blade angle position in real and virtual model and always to have control parameters for adjusting appropriate blade angle (figure 3a and b). It is possible with two points on leading and trailing edge of the profile at the external diameter (figure 3b).

Other geometry relations like cylindrical cuts on characteristic diameters for controlling profiles distribution along the blade or gap between blade external diameter and

hub or housing, or else, can also be checked. This fan CAD model was also used for performing CFD calculations, what was not reported here.

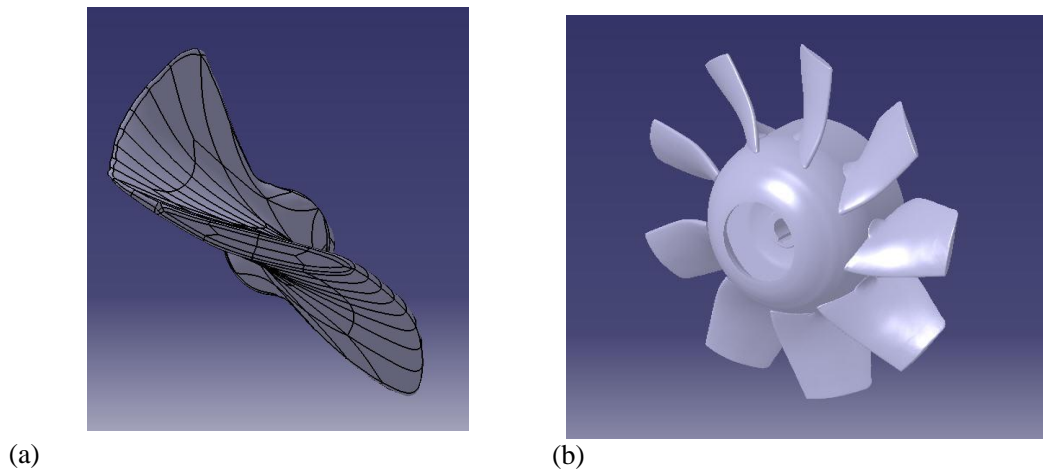


**Figure 2. a) Scanned impeller blade. Imported to the software CATIA; b) Modeled axial fan impeller geometry**

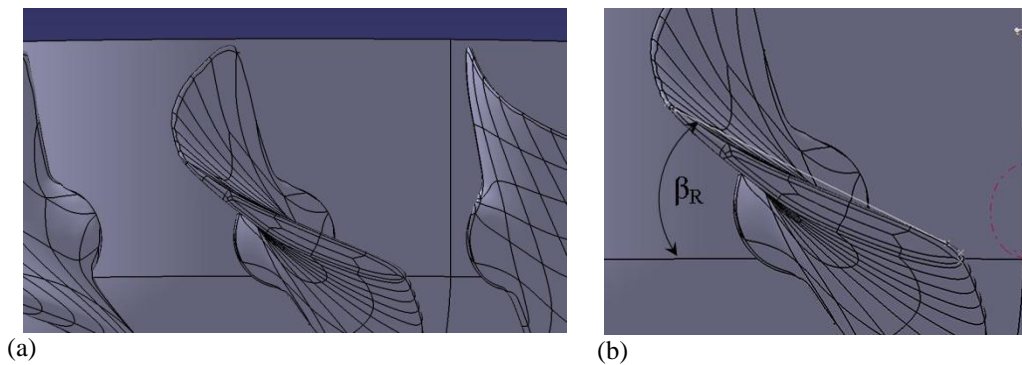


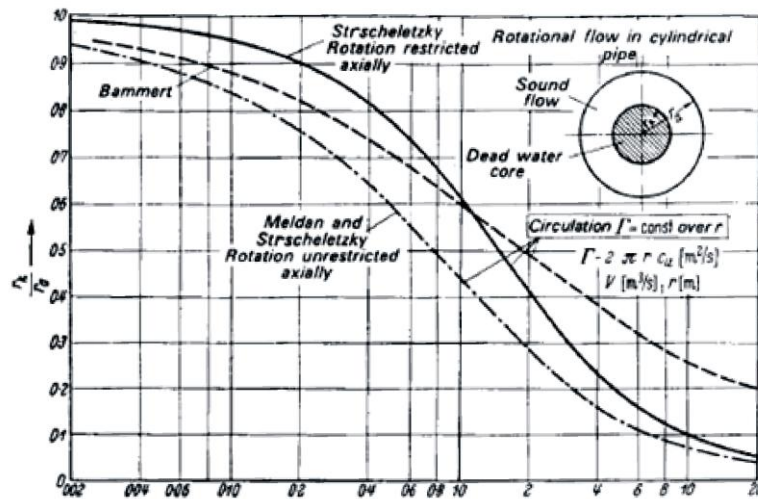
**Figure 3. a) Impeller blade cascade. b) Impeller blade angle check**

### ***3-D axial turbomachine modeling software***

There are various methods for designing axial turbomachines. Developed 3-D axial turbomachines modeling software is based on the modified Weinig-Eckert method, introduced by Protić<sup>†</sup>. Design of the axial turbomachines depends much on the way in which it will be built in. Project parameters depend on what is behind the axial fan impeller like outlet vanes, diffuser, elbow, combination of all of them, *etc.*

Software is based on the optimum correlation between the fan geometry and the optimum coefficients. Some conditions should be fulfilled for specific dimensionless characteristics.

Optimal empirical relation between volume coefficient and pressure coefficient is introduced by Strscheletzky [8 – 10] (figure 4). Selection of the smallest hub diameter of axial flow fans is based on these relations.



$$\frac{c_m}{c_u} = \frac{2\varphi}{\psi_{th}} = \frac{\dot{V}}{\Gamma r_a}; \left[ c_m = \frac{\dot{V}}{\pi r_a^2} \right] \rightarrow \frac{\varphi}{\psi_{th}} = \frac{2(1 - v_k^2)}{\psi_{th}} \text{ (Axially restricted);}$$

$$\frac{\varphi}{\psi_{th}} = \frac{1}{2} \sqrt{\frac{1}{2v_k^2} (1 - v_k^2)^2 - (1 - v_k^2)^2} \ln v_k^2 \text{ (Axially unrestricted)}$$

Figure 4. Strscheletzky boundary layer conditions of the hub dead space [10]

Two equations are defined, for restricted and axially unrestricted swirl flow. The discussed fan was designed to work with outlet vanes what is the case of axially restricted swirl flow.

Coefficients for characterization of each hydraulic element are introduced in order to attain maximum energy efficiency coefficient. On the basis of the performed investigations losses in the impeller, stay vane, diffuser, *etc.* are determined [10]. In this way optimal calculation procedure is obtained.

Calculation of the flow kinematics is based on the uniform inflow and on the constant circulation law  $rW = \text{const}$ . This velocity distribution was proved by measurements with classical probes and LDA measurements behind the axial fan impeller.

Algorithm based on the optimum calculation procedure was programmed in MatLAB with data exporting to *.xls* format and afterwards importing to CATIA software where the 3-D model was formed.

Software will enable choosing of various families of airfoils in cylindrical sections along the blade, as well as appropriate coefficients. Advanced tools, based on mathematically defined criteria, enable smooth surface shaping.

In figure 5a four characteristic profiles along the blade axis are shown. Profile overlapping is also checked (figure 5b). One should be very careful when comparing these

two blades as the scanned blade is not result of CNC machining, but hand machined casting. The second one is precisely computer modeled blade.

The software is also tested in work with axial pumps where also provided good results and it is accepted as a technical solution.

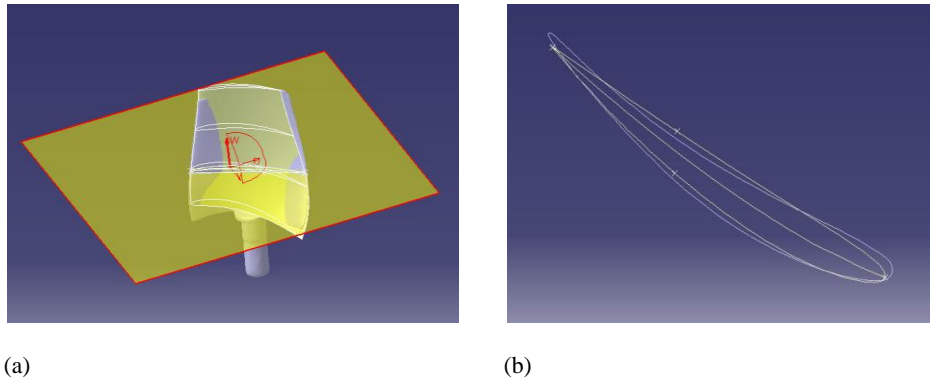


**Figure 5.**  
*a) Overlapping of scanned and software modeled blades. Section with plane normal to the one with blade axis; b) Profile overlapping in the section plane*

### Axial fan operating characteristics

Axial fan operating characteristics were measured on the standardized test rig (ISO 5801) in the Laboratory for Hydraulic Machinery and Energy Systems, Faculty of Mechanical Engineering, University of Belgrade (figure 6). There are few standardized ways to experimentally determine axial fans operating characteristics.

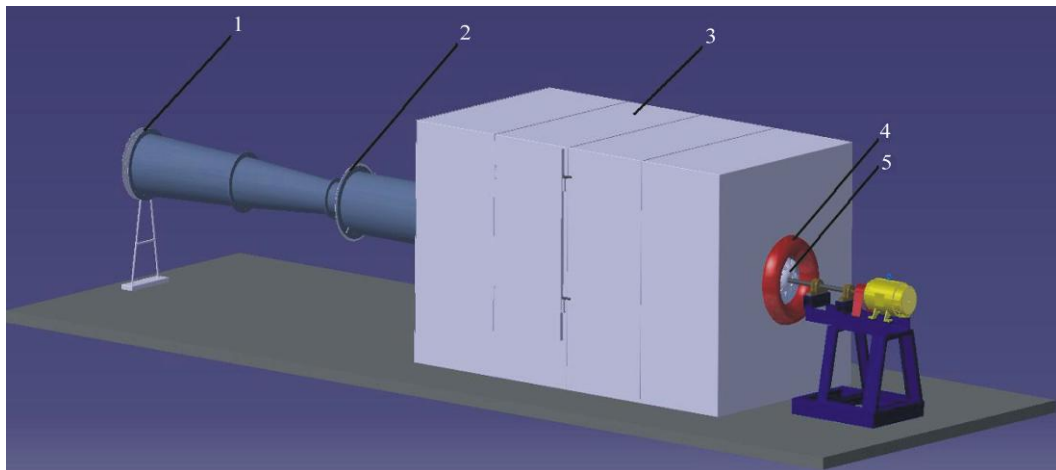
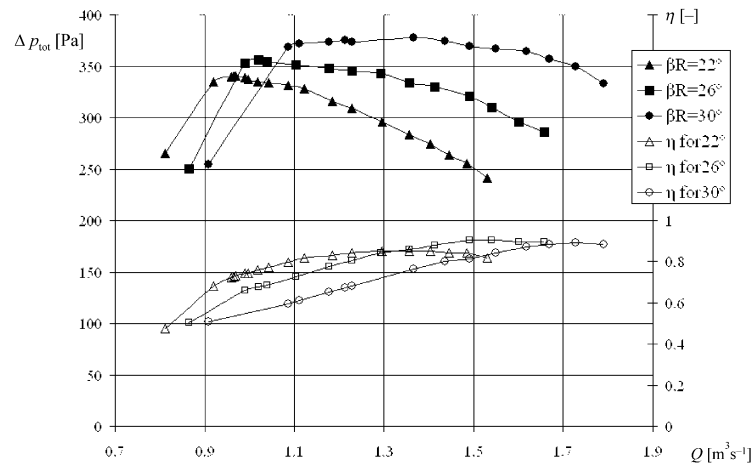


**Figure 6. Standardized test rig (ISO 5801)**  
*(1) – volume flow rate regulation and outlet, (2) – nozzle for volume flow rate measurement, (3) – closed chamber, (4) – profiled free bell-mouth inlet, (5) – tested axial fan impeller*

Here is presented an installation where the axial fan was tested with outlet vanes, in the formation free inlet and free outlet. The installation is shown with motor carrier made of steel profiles. Soon after these experiments concrete one was installed for solving vibrations problem. Booster fans are added, for wider range of operating characteristics.

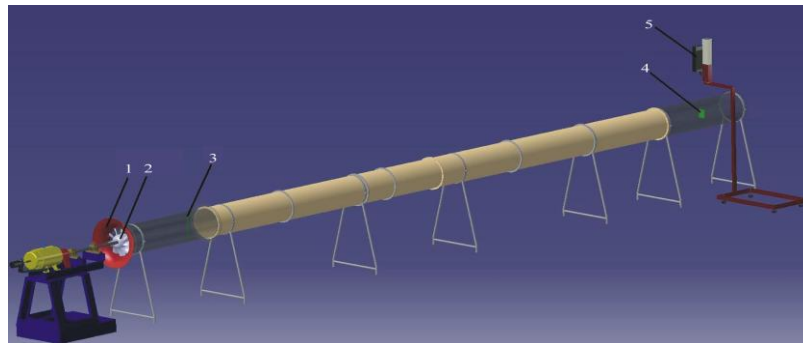
**Figure 7. Results of the operating characteristics on the standardized test rig (ISO 5801) for the first model of outlet vanes for  $n = 1850$  rpm**



### PIV and LDA measurements of the turbulent swirl flow field

Axial fan was tested for constant rotational speed  $n = 1850$ rpm, for various impeller blade angles  $\beta_R = 22^\circ$ ,  $26^\circ$  and  $30^\circ$  and for three types of outlet vanes. Nine various combinations were generated. Here are presented results only for the first type of outlet vanes, what, in combination with impeller, resulted in optimum fan model (figure 7). Optimum blade impeller position,  $\beta_R = 26^\circ$ , was determined on the basis of these results which agree with designed parameters.

**Figure 8. Experimental facility**  
 (1) – profiled free bell-mouth inlet, (2) – swirl generator (axial fan), (3) – LDA measuring section, (4) – PIV measuring section, (5) – Nd:Yag laser for PIV



Axial fan was, afterwards, positioned in a straight circular pipe for investigating swirl turbulent flow behind it (figure 8). Pipe has inner diameter  $D = 0.4$ m. It has two

transparent sections, one, at the inlet, 1.5m long, and one at the outlet 1.38m long. Two plastic, nontransparent, pipe sections are 4m each long. Therefore, total length of the installation is  $L = 27.2 \cdot D$ . Test rig configuration can be varied depending on the measurements needs.

Impeller blade angle was  $\beta_R = 22^\circ$ . Fan rotation speed was regulated by a fully automated thyristor bridge with error up to  $\pm 0.5$ rpm. The fan shaft speed has been measured by photo cell. Axial fan has DC electric motor, with 5kW power.

### PIV measurements

Some stereo PIV measurements were previously performed and discussed in papers [11, 12]. Correlation functions, probability distributions and statistical moments of the higher order, which are determined experimentally by the use of hot-wire anemometry, together with PIV results, point out, very specific phenomena and transport processes in the core region and turbulent shear flow in pipe swirl flow [11].

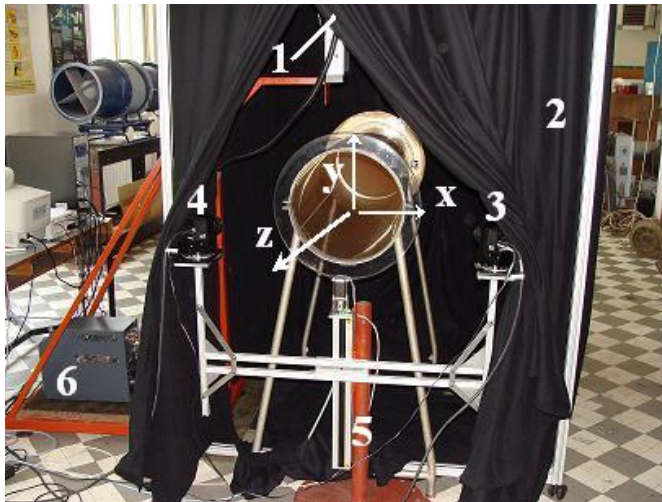


**Figure 9. Experimental facility with the PIV system set up for measurements in pipe's cross-section**

(1) – Nd:Yag laser with computer controlled linear guide, (2) – chamber, (3) – right CCD camera, (4) – left CCD camera, (5) –  $\Pi$ -shaped camera carrier positioned on computer controlled linear guide, (6) – laser power supply

PIV measurements were performed in the section  $L=25.75 \cdot D$  in the middle of the pipe cross section, region 100x120mm (figure 9).

A commercially available Stereoscopic PIV system manufactured by TSI Inc (Shoreview, USA) has been used for flow visualizations and the extraction of velocity fields. The system consists of a 15Hz dual Nd: Yag laser (New Wave Research, Solo PIV, max power: 30mJ/pulse, wavelength 532nm), synchronization unit, proper optics for the formation of the planar light sheet, two 12-bit CCD cameras with resolution of 1660x1200 pixels and the TSI Insight 3G processing software. On the Nd: YAG laser was mounted cylindrical lens with focal length of – 15mm and one spherical lens with focal length 500mm.

Stereo PIV measurements were conducted in pipe's cross-section, *i. e.* x-y plane (figure 9) for different shaft speed rotations that span the range of 500 to 2500rpm. In figure 9

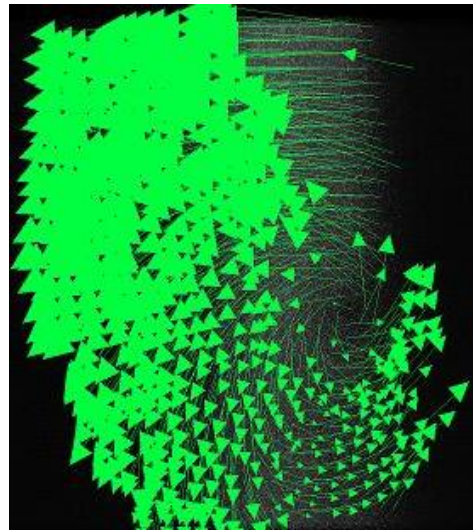


is presented a stereo PIV configuration with two CCD cameras. They have to, together with laser sheet, obey Scheimpflug principle.

Measuring section can be, with PIV system, illuminated by a thin laser sheet (~1 mm in width) while the scattered light is captured by CCD camera. The CCD cameras are synchronized with pulses for the two lasers and the timing between the two laser flashes is varied depending on the flow velocity. The fluid flow is seeded with olive oil drops, of an average diameter 0.6 $\mu$ m and a reflection coefficient 1.47, generated by six-jet atomizer positioned at the axial fan free inlet.

The vector fields (shown in the results section) have been determined using TSI INSIGHT 3G PIV processing software which implements different processing schemes. For the measurements taken in the cross-section plane x-y plane (figure 9) the Central difference image correction (CDIC) deformation algorithm [13] combined with the Hart correlation [14] method was used (figure 10).

**Figure 10. A close-up of the velocity vectors processing using deformation processing scheme for the case  $n = 2500$  rpm (CDIC, [14])**



This four-pass method employed an interrogation region of  $32 \times 32$  px<sup>2</sup> with 75% overlap (final size). The vector fields were validated using standard velocity range criteria and a  $3 \times 3$  local median filter. Finally, any missing vectors were interpolated using a  $3 \times 3$  local mean technique. The number of spurious vectors was, in average, less than 6%. The processing algorithm maintains a spatial displacement accuracy of less than approximately 0.1 px, so that the spatial displacement error is on the order of less than 2.5% for a particle displacement of four pixels. The error associated with temporal variations in the laser pulse synchronization due to the jitter of the electronics is negligible since it is several orders of magnitude smaller [15].

Results for the swirl flow generated by axial fan are presented in figure 11. These PIV images have been obtained by averaging 300 pictures obtained in a sequence with maximum laser working frequency 14.5 Hz for various rotational speeds.

It is obvious that the averaged speed is changed by varying fan rotational speed as the volume flow rate is changed. Averaged position of the vortex core is also changed by varying rotational speed, but much less than in the case of some other tested fans. Obtained results show high level of activity, turbulence intensity, what is obvious in a pipe's cross-section, and especially dominant for specific volume flow rates.

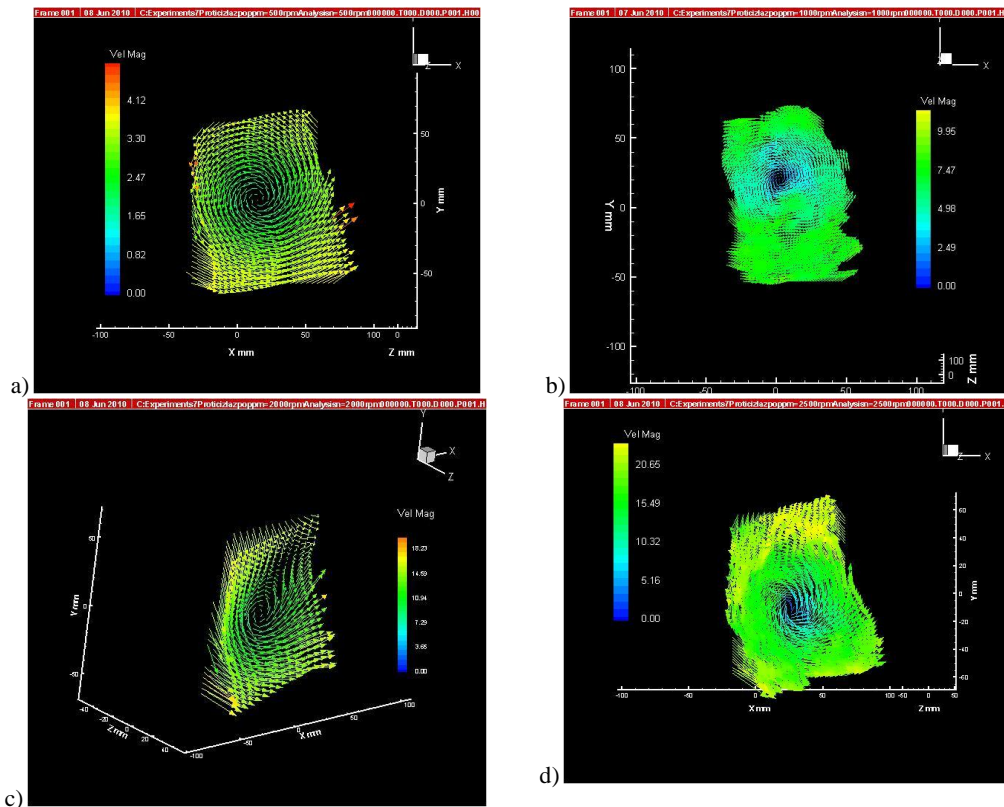


**Figure 11.** Averaged velocity fields for specified rotational speeds  
 (a)  $n = 500$  rpm, (b)  $n = 1000$  rpm, (c)  $n = 2000$  rpm and (d)  $n = 2500$  rpm

### LDA measurements

LDA measurements were performed along the vertical diameter in section  $L = 3D$  in points on 10 mm distance each. First two points, on 10 mm distance from the inner wall, are omitted. Corrections for LDA measurements, considering wall curvature, are also calculated.

Commercially laser anemometer equipment available was used. It was Dantec model FlowExplorer Mini LDA with BSA F30 signal processor model with measurement distance at 285 mm, power 35 mW, measurement volume diameter 0.1mm, measurement volume length 1mm and maximum velocity  $27 \text{ ms}^{-1}$ . Laser has great flexibility thanks to its size  $98 \times 98 \times 396$  mm, weight of 5 kg and compactness. It works in backscattered mode. Unfortunately,

available system was one-component and all three velocity components had to be measured separately. Velocity is measured with uncertainty lower than 0.1%. Traverses were designed to measure them in the same points (figure 12).

In figure 12 are presented test rigs for measuring all three velocity components. Tracers were obtained from modified fog generator Hurricane 1700, Chauvet and system of plastic pipes for accumulation and fog distribution (figure 12.b). This was the way to obtain enough tracers for needed sampling rate of more than 6 kHz. It was possible to obtain, in some positions, more than 11 kHz. With six-jet atomizer and olive seeding maximum acquisition sampling rate was only few kHz. Used fluid was eucalyptus extract.



**Figure 12. Test rig for LDA measurements**

*a) circumferential velocity component: (1) – laser, (2) – computer controlled linear guide, (3) – profiled bell – mouth inlet, (4) – swirl generator, (5) – seeding; b) axial and radial velocity components: (1) – laser, (2) – seeding distribution, (3) – fog generator, (4) – photo-cell*

Distribution of only time averaged values of axial and circumferential velocity components for all five regimes are presented in the following figures, (figures 13 and 14), respectively. Axial velocity distribution is characteristic for turbulent swirl flows. Circumferential velocity distribution show characteristic distribution for combined swirl flow profile. In the center zone is visible a core region with solid body profile and in the sound flow region is potential flow ( $rW = \text{const.}$ ), what was designed. It is also evident that region of potential flow is greater than the hub diameter what was also expected as it was designed in this way. One of the main reasons for generating this kind of profile immediately at the fan outlet is a fact that all the profiles will be transformed into this one along the pipe, but with energy dissipation.

It is evident from figures 13 and 14 that flow is axisymmetrical with a little displacement of the minimum from center. Turbulence signals, especially in the core region, show great dynamics of the flow what is in accordance with PIV results. These measurements are of great significance, as the ones with classical probes revealed problems with

measurements in the core region. Discussion of the turbulent signal, obtained for each point in the section is not presented in this paper.

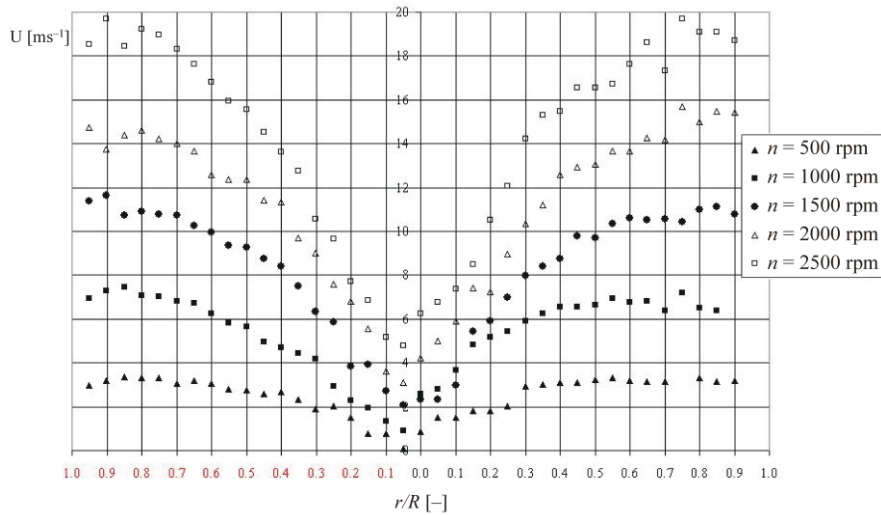


**Figure 13.**  
Distribution of the time averaged axial velocity component along the vertical diameter in section  $L = 3D$

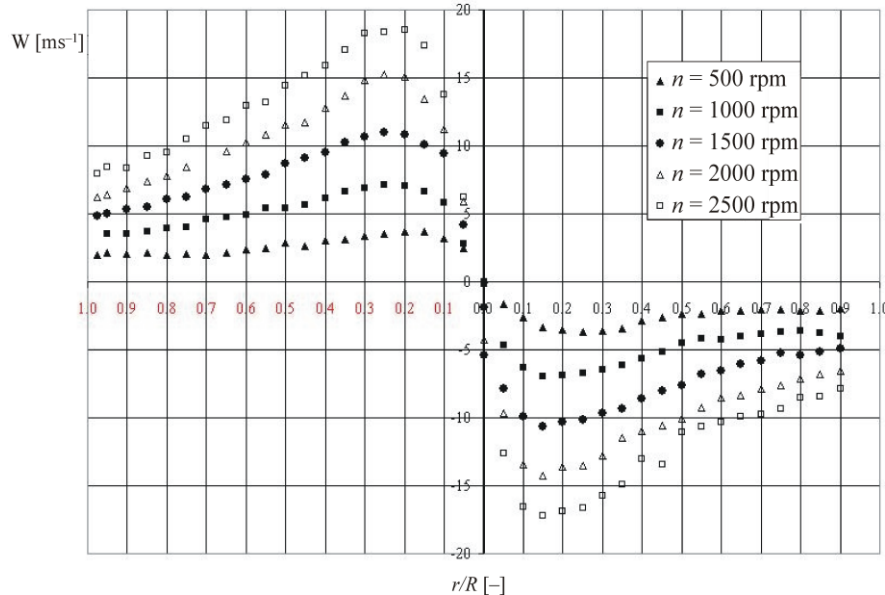
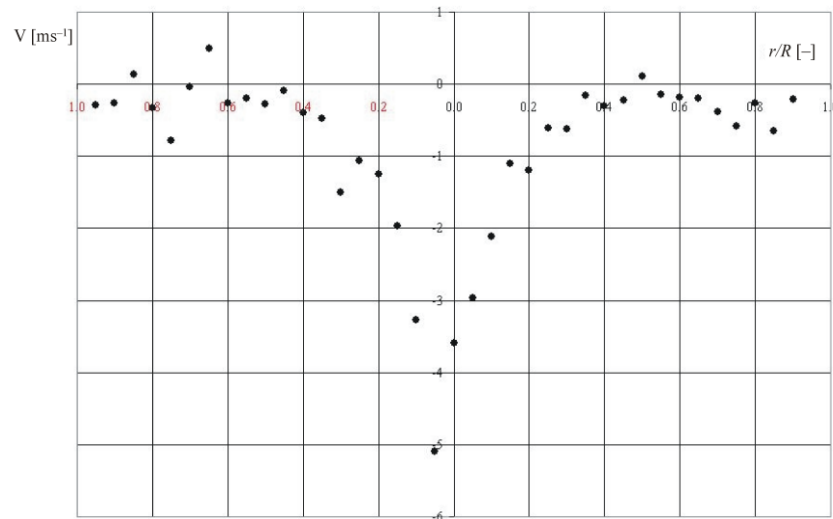


**Figure 14.**  
Distribution of the time averaged circumferential velocity component along the vertical diameter in section  $L = 3D$

Distribution of the radial component (figure 15) reveals something new, as till know this component was mainly omitted. It is a fact that radial velocity component has small value for the most of the cross section, but, it has, also values of almost the same magnitude as other

components in the core region. This was almost impossible to be testified with classical probe measurements. Presented radial velocity distribution for rotational speed  $n = 1000$  rpm, is almost symmetrical along diameter.

**Figure 15.**  
Distribution of the  
time averaged radial  
velocity component  
along the vertical  
diameter in section  
 $L = 3D$  for  
 $n = 1000$  rpm



This was repeated for other rotational numbers. This enlightens complex energy, mass and momentum exchange processes in this complex fluid flow. Turbulent swirl flows are very specific phenomena in complex and intensive transport processes especially in the core region and turbulent shear flow.

## Conclusions

An axial fan designing and turbulent swirl flow phenomenon occupies attention of many researchers in scientific laboratories and industry, as it has significant influence on fluid transport processes, energy efficiency, *etc.*

It is demonstrated how modern scanning techniques and software skills, coupled together, offer good results and flexibility in optimal designing process.

Swirl flows are very dominant in applied technical problems, especially in hydraulic machinery. Their prediction requires rather sophisticated modeling. Physical understanding of this phenomenon would enlighten many unsolved problems and help developing new turbulent numerical models for CFD analysis.

The purpose of the reported PIV and LDA measurements is to document swirl flow field and its vortex core kinematics at different volume flow rates, *i. e.* various Reynolds numbers and swirl intensities. Velocity magnitude of total velocity and each component separately are documented. The magnitude and gradient of radial velocity component in the core region is evident.

In the planned future research impeller blade angles will be changed and some commercial axial fans will be introduced. Measurements were made in a pipe cross-section

and for future ones in a meridian section (plane z-y, figure 9). Discussion of statistical values, based on LDA measurements, will be implemented in the future papers.

Obtained qualitative and quantitative visualization and measurement results give closer insight into physics of complex flow processes in the swirl flow. Performed and planned investigations will make possible, not just testing, but also development of the new models for this class of very complex turbulent fluid flows. It is expected that results would reveal precession and kinematics of the swirl flow core.

### Acknowledgment

This work was funded by grants from the Ministry of Science and Technological Development, Republic of Serbia (TR 14046). The Government of the Republic of Serbia and the Ministry of Science and Technological Development have provided the fund for capital equipment investments in science, including this PIV and LDA system, as a part of the National Investment Programmed in 2006/2007. We are grateful for their support of great significance. Authors express their gratitude, also, to the company 3-D set from Belgrade and its director Mr. Zoran Miljenović, Dipl.-Ing. Mr. Slobodan Todorović and Vlada Miljenović who helped them to perform 3-D scanning of the fan impeller blade.

### In memoriam

Our much appreciated Prof. Dr.-Ing. Zoran D. Protić (1922 – 2010) passed away on the 24<sup>th</sup> of April 2010. in the time of active work on this paper. We owe him our deepest gratitude for everything he has done, during all these years of his dedicated work, in scientific, engineering and human way, for developing and applying science of hydraulic machines, energy systems and applied fluid mechanics in the Republic of Serbia.

### Nomenclature

|     |   |                      |  |
|-----|---|----------------------|--|
| $U$ | – time averaged axial velocity component, [m/s]           | $V$                  | – time averaged radial velocity component, [m/s] |
| $W$ | – time averaged circumferential velocity component, [m/s] | $L$                  | – length along the z-axis (pipe axis), [m]       |
| $n$ | – fan shaft rotation speed, [rpm]                         | <i>Greek letters</i> |  |
| $D$ | – pipe inner diameter, [m]                                | $\beta_R$            | – impeller blade angle, [°]                      |

### References

- [1] Protić Z., Determination of the Dead Water Diameter in Swirl Turbulent Flow in Straight Circular Pipes, (in Serbian), *Proceedings*, 10<sup>th</sup> Yugoslav Congress of Rational and Applied Mechanics, Baško Polje, Yugoslavia, 1970, pp. 429-442
- [2] Protić, Z., Benišek, M., Determination of System Characteristics at Swirling Flow in a Duct Connected with a Fan without Straightening Vanes, (in Serbian), *Proceedings*, 15<sup>th</sup> Yugoslav Congress of Rational and Applied Mechanics, Kupari, Yugoslavia, 1981, B-27, pp. 361-368
- [3] Benišek, M. H., Investigation of the Turbulent Swirling Flows in Straight Pipes, (in Serbian), Ph. D. thesis, Faculty of Mechanical Engineering, University of Belgrade, Belgrade, 1979

- [4] Čantrak, S., Experimental Investigation of the Statistical Properties of Swirling Flows in Pipes and Diffusers, (in German), Ph. D. thesis, Faculty of Mechanical Engineering, Technical University Karlsruhe, Karlsruhe, Germany, 1981
- [5] Lečić, M. R., Theoretical and Experimental Investigations of the Turbulent Swirling Flows (in Serbian), Ph. D. thesis, Faculty of Mechanical Engineering, University of Belgrade, Belgrade, 2003
- [6] Čantrak, S., *et al.*, Problems of Non-Local Turbulent Transfer Modeling, (in German), *ZAMM*, 81 (2001), S4, pp. 913-914
- [7] Čantrak, S. M., Benišek, M. H., Characteristic Magnitudes Determined from Mean Velocity Distributions of Turbulent Swirling Flow in Pipes, *ZAMM*, 62 (1982), 4, pp. 201-203
- [8] Strscheletzky, M., A Contribution to the Theory of the Fluid Flow Hydrodynamic Equilibrium, (in German), *Voith-Forsch und Konstrukt.*, 2 (1957), 1, pp. 1-8
- [9] Strscheletzky, M., Kinetic Balance Method of the Inner Incompressible Fluid Flows (in German), *VDI-Z Fortschritt Berichte* 7, (1961), 21, pp. 113-132
- [10] Eck, B., Fans, Pergamon Press, London, 1975
- [11] Čantrak, Dj., *et al.*, PIV Measurements and Statistical Analysis of the Turbulent Swirl Flow Field, *Proceedings on CD, ISFV 13 – 13<sup>th</sup> International Symposium on Flow Visualization, FLUVISU 12 – 12<sup>th</sup> French Congress on Visualization in Fluid Mechanics, Nice, France, 2008, ID 183 – 0804203*
- [12] Ilić, J., Čantrak, Dj., Srećković, M., Laser Sheet Scattering and the Cameras' Positions in Particle Image Velocimetry, *Acta Physica Polonica A*, 112 (2007), 5, pp. 1113-1118
- [13] Wereley, S.; Gui, L., A Correlation-based Central Difference Image Correction (CDIC) Method and Application in a Four-roll Mill Flow PIV Measurement, *Experiments in Fluids*, 34 (2003), pp. 42-51
- [14] Hart, D. P., PIV Error Correction, *Experiments in Fluids*, 29 (2000), 1, pp. 13-22
- [15] Adrian, R., Dynamic Ranges of Velocity and Spatial Resolution of Particle Image Velocimetry, *Meas. Sci. Technol.*, 8 (1997), pp. 1393-1398

